DOI: 10.1002/ejoc.200700414

Thermochromism at Room Temperature in Overcrowded Bistricyclic Aromatic Enes: Closely Populated Twisted and Folded Conformations

Amalia Levy,[a] Sergey Pogodin,[a] Shmuel Cohen,[a] and Israel Agranat*[a]

Keywords: Thermochromism / Strained molecules / Conformation analysis / Density functional calculations

The overcrowded thermochromic bistricyclic aromatic enes (BAEs) 10-(9′*H*-fluoren-9′-ylidene)-9(10*H*)-anthracenone (**6**), 10-(11′*H*-benzo[*b*]fluoren-11′-ylidene)-9(10*H*)-anthracenone (**7**), and 10-(1′,8′-diaza-9′*H*-fluoren-9′-ylidene)-9(10*H*)-anthracenone (**8**) were synthesized by applying Barton's two-fold extrusion diazo-thione coupling method and their crystal and molecular structures were determined. BAEs **6**–**8** exhibit thermochromic behavior at room temperature due to the equilibrium between the yellow *anti*-folded conformations and the thermochromic purple, blue, or red twisted conformations. The NMR experiments demonstrate a fast interconversion of the twisted and the *anti*-folded conformers of **6**–**8** in solution. BAE **7** readily undergoes *E*,*Z*-topomerization at room temperature with the coalescence point at 297 K and the relatively low energy barrier of $\Delta G_c^{\ddagger}(\mathbf{t}_\perp)$ = 65.5 kJ/mol. B3LYP/6-311++G(d,p) calculations predict *anti*-folded **a-6** and **a-7** to be less stable than twisted **t-6** and **t-7** by 0.8 and 1.3 kJ/mol, respectively, whereas **a-8** is more stable than **t-8** by 10.7 kJ/mol. DFT calculations of **6**–**8**, 9-(9′*H*-fluoren-9′-ylidene)-9*H*-fluorene (**1**), [10′-oxo-9′(10′*H*)-anthracenylidene]-9(10*H*)-anthracenone (**2**) and their 1,8-diaza-substituted derivatives show that substitution in the fluorenylidene unit destabilizes the twisted conformations by 11–22 kJ/mol, while introduction of nitrogen atoms at the 1 and 8 positions of anthracenylidene unit destabilizes the *anti*-folded conformations by 14–18 kJ/mol.

Introduction

Bistricyclic aromatic enes (BAE, Figure 1) are attractive substrates for the study of the conformational behavior and dynamic stereochemistry of overcrowded polycyclic aromatic enes and for the interplay of strain and delocalization effects.[1] The leading member of the family, red 9-(9′*H*-fluoren-9′-ylidene)-9*H*-fluorene (bifluorenylidene, **1**) was synthesized in 1875.[2] BAEs can be classified into *homomerous* bistricyclic aromatic enes (Figure 1, X = Y) and *heteromerous* bistricyclic aromatic enes (Figure 1, X ≠ Y). The phenomenon of thermochromism,[3–5] – reversible change of color with change of temperature – was revealed in overcrowded BAEs almost five scores years ago.[6] Meyer reported that yellow solutions of 10-[10′-oxo-9′(10′*H*)-anthracenylidene]-9(10*H*)-anthracenone (bianthrone, **2**) reversibly turn dark green upon heating.[6] This change of color may also be triggered by pressure (piezochromism)[7] or by UV irradiation at low temperatures (photochromism).[3d,8] Thermochromic and photochromic BAEs and related overcrowded enes serve as candidates for chiroptical molecular switches and molecular motors.[9] Derivatives of **2** are topologically related to hypericin, widespread in St. Johns Wort, an important remedy against depression.[10] A tetradehydrodianthracene unit, also topologically related to **2**, is a beltlike pyramidalized component of the first Möbius annulene.[11]

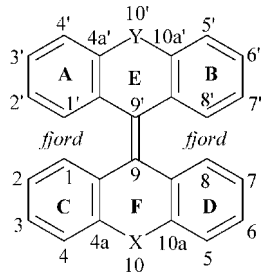

Figure 1. Bistricyclic aromatic enes.

Thermochromism in BAEs has been attributed to a unimolecular equilibrium between two distinct and interconvertible conformers: a colorless or yellow ambient-temperature form **A** and a deep-blue or deep-green high-temperaceture form **B**:[12]

$$A \overset{kT}{\rightleftharpoons} B$$

Although A absorbs in the UV region (and close to it), the thermochromic form has a new absorption band at $\lambda \approx$ 600–700 nm. In thermochromic BAEs, the enthalpy differ-

[a] Department of Organic Chemistry, The Hebrew University of Jerusalem, Jerusalem 91904, Israel
E-mail: isria@vms.huji.ac.il
Fax: +972-2-6511907
Supporting information for this article is available on the WWW under http://www.eurjoc.org or from the author.

ence ΔH of the two forms is 4–30 kcal/mol[12] and is independent of the solvent.[12a] The thermochromic, photochromic, and piezochromic **B** forms are identical.[8c,12c,12f,13] Recently the controversial nature of the thermochromic phenomenon in BAEs has been resolved: the deeply colored purple (or green) thermochromic form **B** was identified as the twisted conformation, and its molecular structure was reported.[5] The high twist in the central double bond reduces the π-overlap and causes a substantial red shift. The yellow or colorless ambient-temperature form **A** was identified as *anti*-folded or unevenly *anti*-folded conformations.

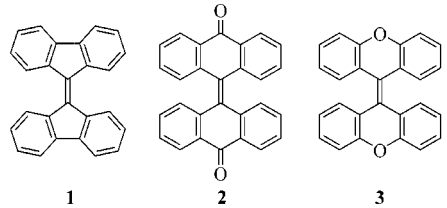

1 **2** **3**

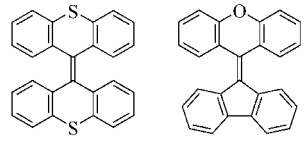

4 **5**

Three types of conformational behavior have been distinguished in BAEs.[14] The necessary conditions for the thermochromism of the Type 1 BAEs are a global minimum *anti*-folded **a** or unevenly *anti*-folded **au** conformation corresponding to the room temperature form **A**, a low energy local minimum twisted conformation **t** corresponding to the thermochromic form **B**, and an energy difference between these conformations which is sufficiently small to allow thermal population of **t**, i.e. less than 30 kJ/mol, based on experimental data and DFT calculations.[14] Examples of Type 1 BAEs are bianthrone (**2**) and 9,9′-bi-9*H*-xanthen-9-ylidene (dixanthylene, **3**). BAEs of Type 2 also adopt *anti*-folded conformations as global minima, but their *syn*-folded conformations **s** are more stable than the twisted conformations, which cannot be populated in thermal equilibrium. Therefore, Type 2 BAEs, for example, 9,9-bi(9*H*-thioxanthen-9-ylidene) (**4**), do not exhibit thermochromic behavior. BAEs of Type 3 adopt twisted conformations as their global minima. Their thermochromic forms dominate in the equilibrium at all temperatures and are responsible for the deep color of these compounds. 9-(9′*H*-fluoren-9′-ylidene)-9*H*-xanthene (fluorenylidene-xanthene, **5**), which has a deep purple color in solution, belongs to Type 3. The folded conformations of Type 3 BAEs, although higher in energy than the twisted conformations, may be populated in equilibrium, but their color is masked by the deeply colored twisted conformations. Packing effects may also favor the folded conformations.[15]

Altering the relative stabilities of twisted and folded conformations of a BAE would result in a change of its conformational space and physical properties, including thermochromism. One of the ways to affect the balance between conformations is to replace the *fjord* regions C^1 and C^8 atoms of one tricyclic moiety of a BAE by nitrogen atoms. Having a van der Waals radius of 150 pm, which is considerably shorter than that of carbon, 171 pm,[16] and not bearing hydrogens, nitrogen atoms at the 1 and 8 positions would render the *fjord* regions of the 1,8-diaza BAE less overcrowded. The *fjord* nitrogens may also affect the BAE molecule in other ways. BAEs with two different tricyclic moieties, like fluorenylidene-xanthene (**5**), have a potentially push-pull character, in which the fluorenylidene may serve as a acceptor, while the xanthylidene or the anthracenylidene moieties may serve as donors.[17] The 1,8-diazofluorenylidene moiety may amplify this effect.[17] By contrast, 10-(9′*H*-fluoren-9′-ylidene)-9(10*H*)-anthracenone (fluorenylidene-anthrone, **6**) is a "pull-pull" system; its fluorenylidene and anthrone moieties are polarized in the same direction.

Here, we report syntheses and molecular and crystal structures of thermochromic BAEs fluorenylidene-anthrone (**6**), 10-(11′*H*-benzo[*b*]fluoren-11′-ylidene)-9(10*H*)-anthracenone (**7**) and 10-(1′,8′-diaza-9′*H*-fluoren-9′-ylidene)-9(10*H*)-anthracenone (**8**), a DNMR spectroscopic study of **7**, as well as a DFT study of the conformational spaces of diaza and tetraaza substituted BAEs. The crystal and molecular structure of **6** has previously been reported.[1a,18]

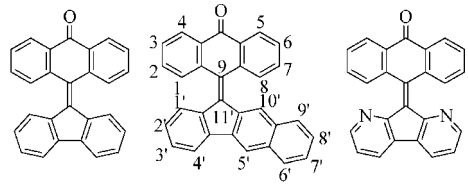

6 **7** **8**

Results and Discussion

Synthesis

BAE **6** was first synthesized in two steps by a condensation between 9,9′-dichloro-9*H*-fluorene and 9-(10*H*)-anthrone in boiling benzene to give 9′-chloro-9*H*′-fluorenyl-9-anthrone followed by heating the latter in boiling nitrobenzene.[19] An attempted synthesis of **6** in one step by a similar condensation between 9,9′-dichloro-9*H*-fluorene and 9-(10*H*)anthrone at 160 °C without solvent, according to a literature procedure[20] afforded **6**, but in unsatisfactory yield and low purity. Therefore, BAEs **6**–**8** were synthesized by applying Barton's twofold extrusion diazo-thione coupling method.[21] Two synthetic routes can be pursued for the preparation of **6**: coupling between 9-diazofluorenone[22] (**9**) and 9-thioxoanthracenone[23] (**10**), or, alternatively, coupling between 9-fluorenonethione[24] (**11**) and 9-diazoanthracenone[23,25] (**12**) (Scheme 1).

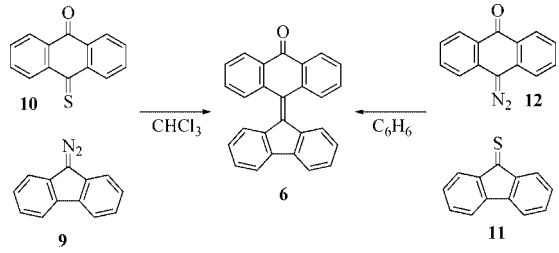

Scheme 1.

The diazo-thione coupling between diazo **9** and thione **10** in boiling $CHCl_3$ gave BAE **6** in 46% yield and appears to be the preferred method for the synthesis of **6**. The alternative coupling between diazo **12** and thione **11** in boiling benzene afforded BAE **6** in 33% yield. The intermediate product of Barton's twofold extrusion, thiirane **13**, can be isolated by the reaction between diazo **9** and thione **10** in CH_2Cl_2 at room temperature (Scheme 2). Heating thiirane **13** in boiling benzene with PPh_3 afforded BAE **6** in 23% yield.

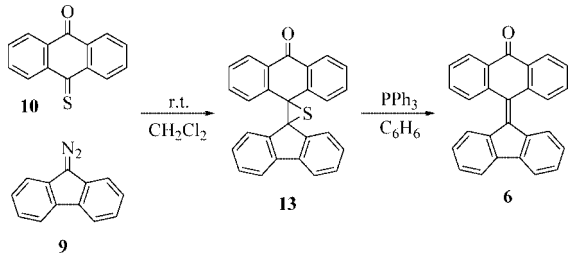

Scheme 2.

10-(11′*H*-benzo[*b*]fluoren-11′-ylidene)-9(10*H*)-anthracenone (**7**), a napthologue of **6**, was prepared by the diazo-thione coupling between 9-diazobenzo[*b*]fluorenone[26] (**14**) and thione **10** in boiling $CHCl_3$ (Scheme 3).

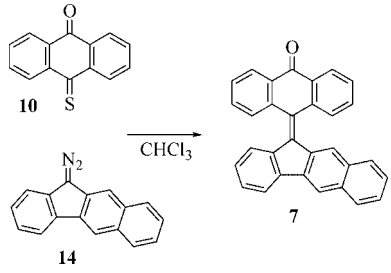

Scheme 3.

1,8-Diazafluorenylidene-anthrone (**8**) was prepared by Barton's diazo-thione coupling method in two steps (Scheme 4). The coupling between 1,8-diaza-9-diazofluorenone[17,27] (**15**) and thione **10** in CH_2Cl_2 at room temperature gave thiirane **16**. Sulfur extrusion from **16** with PPh_3 in boiling benzene afforded BAE **8**.

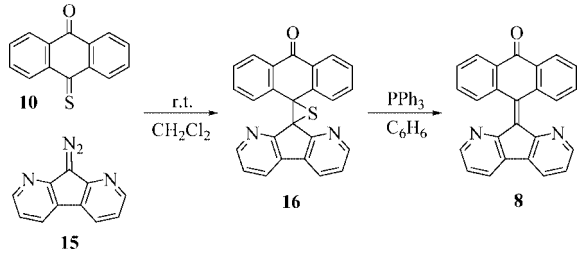

Scheme 4.

In BAEs **6**–**8** there is a subtle equilibrium between the yellow *anti*-folded conformation and the thermochromic deeply colored twisted conformation at room temperature. Fluorenylidene-anthrone (**6**) is yellow in the solid state, but turns purple in solution (UV/Vis spectra has a visible absorption at 546 nm). The greenish-yellow crystals of 10-(11′*H*-benzo[*b*]fluoren-11′-yildene)-9(10*H*)-anthracenone (**7**) give a blue solution with the visible absorption at 590 nm. 1,8-Diazafluorenylidene-anthrone (**8**) is yellow in the solid state and turns dark red in solution (525 nm). The purple, blue, and red colors of **6**–**8** in solution indicate that the twisted conformations of these BAEs (reduced HOMO–LUMO gap) are readily populated at room temperature, while in the solid state, yellow or greenish-yellow color reflects the preference of *anti*-folded conformations.

Molecular and Crystal Structures

BAEs **6** and **8** crystallize in the space group $P2_1/n$. Compound **7** crystallizes in the space group *Pbca*. Figures 2, 3 and 4 give ORTEP diagrams of one molecule of each of BAEs **6**–**8**, respectively, as determined by X-ray analysis (anisotropic displacement parameters are drawn at the 50% probability level). The crystal data of **6**–**8** are given in Table 6.[28] Table 1 gives the conformations and selected geometrical parameters of **6**–**8** derived from the crystal structures and from DFT calculations (vide infra). Pure ethylenic twist[1c] (ω) around $C^9{=}C^{9'}$ is defined as the average of the two torsion angles C^{9a}–C^9–$C^{9'}$–$C^{9a'}$ and C^{8a}–C^9–$C^{9'}$–$C^{8a'}$; folding dihedral of the tricyclic (fluorenylidene or anthracenylidene) moiety (*A*–*B*) and (*C*–*D*), see Figure 1, is defined as the dihedral angle between the least-square planes of the atoms of the benzene rings of each tricyclic moiety and reflecting the non-planarity of the tricyclic moieties; bistricyclic dihedral between the tricyclic moieties (*AEB*–*CFD*) is defined as the dihedral angle between the least-square planes of all the untagged and all the tagged carbon and nitrogen atoms; pyramidalization angles[1c] $\chi(C^9)$ and $\chi(C^{9'})$ are defined as the improper torsion angles C^{9a}–C^9–$C^{9'}$–C^{8a} and $C^{9a'}$–$C^{9'}$–C^9–$C^{8a'}$, minus 180°. The overall conformations of the bistricyclic aromatic enes are characterized by the pure twist of the central $C^9{=}C^{9'}$ bond and by the folding dihedral of the tricyclic moieties.[1b] The pyramidalization angles $\chi(C^9)$, $\chi(C^{9'})$, and $\chi(C^{10})$ should also be considered.[1b]

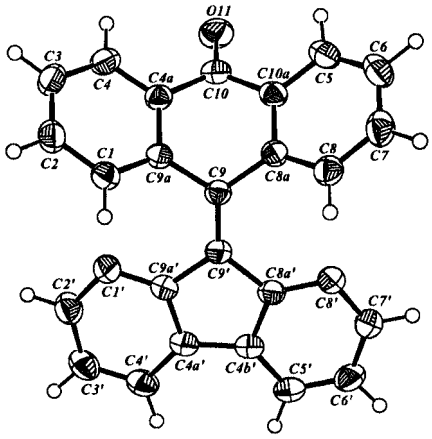

Figure 2. ORTEP drawing of the molecular structure of 10-(9′*H*-fluoren-9′-ylidene)-9(10*H*)-anthracenone (**6**).

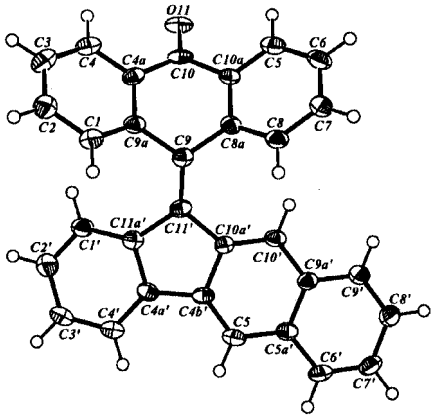

Figure 3. ORTEP drawing of the molecular structure of 10-(11′*H*-benzo[*b*]fluoren-11′-yildene)-9(10*H*)-antracenone (**7**).

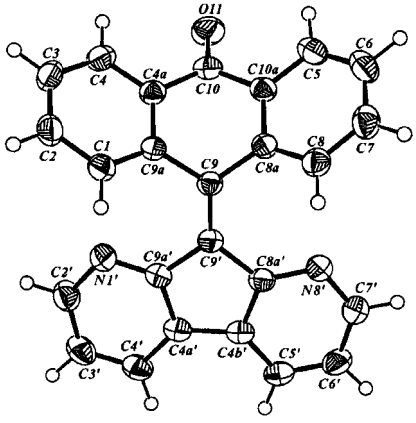

Figure 4. ORTEP drawing of the molecular structure of 10-(1′,8′-diaza-9′*H*-fluoren-9′-ylidene)-9(10*H*)-anthracenone (**8**).

The molecular and crystal structures of BAEs **6**–**8** indicate that these molecules adopt *anti*-folded conformations, which are characterized by small pure twist angles (3.2–3.5°) and significant folding dihedrals. The folding dihedrals of **6** are 51.1° in the anthracenylidene moiety and 11.8° in the fluorenylidene moiety. Only C^9 is pyramidalized (8.5°), while $C^{9'}$ is not. The degrees of overcrowding in the *fjord* regions of **6**, as reflected in the intramolecular distances at the *fjord* regions, $C^1\cdots C^{1'}$, $C^8\cdots C^{8'}$, $C^1\cdots H^{1'}$, and $C^8\cdots H^{8'}$ are significant: 301.7, 309.1, 240.4, and 239.3 ppm. These distances reflect 12, 10, 16, and 16% of penetration, based on the van der Waals radii of carbon and hydrogen which are 171 and 115 ppm.[16] Each molecule of **6** is chiral, and the unit cell of **6** consists of two pairs of enantiomers. The fluorenylidene units of two molecules A and B forming a pair are parallel to each other but orientated in the opposite directions. Their plane makes a dihedral angle of 14° with the *xy* plane of the unit cell. The distance between the planes of the five-membered rings of each fluorenylidene unit is 386.0 pm, and the torsion angle C^9(A)–$C^{9'}$(A)–$C^{9'}$(B)–C^9(B) is 180°.

BAE **7** is also chiral. The unit cell of **7** consists of four pairs of enantiomers. The folding dihedrals of **7**, as compared to those of **6**, are smaller in the anthracenylidene moiety, 43.3°, and larger in the fluorenylidene moiety, 15.8°. Both C^9 (7.4°) and, to a lesser extent, $C^{9'}$ (3.0°) atoms are pyramidalized. Compound **7** is more overcrowded in its *fjord* regions than **6**: the $C^1\cdots C^{1'}$, $C^8\cdots C^{8'}$, $C^1\cdots H^{1'}$, and $C^8\cdots H^{8'}$ distances are 293.2, 302.2, 236.7, and 240.1, corresponding to 14, 12, 17, and 16% of penetration.

The folding dihedrals of **8** are smaller than those of **6**, 47.5° in the anthracenylidene moiety and 7.5° in the fluorenylidene moiety. Both C^9 (7.4°) and $C^{9'}$ (4.9°) atoms are pyramidalized. The introduction of nitrogen atoms in the *fjord* region of **8** eliminates short C···H distances, but **8** is still overcrowded, its $N^1\cdots C^{1'}$ and $N^8\cdots C^{8'}$ distances are 278.1 pm (13.4% penetration) and 286.9 pm (11% penetration). The unit cell of **8** consists, as in the case of **6**, of two pairs of enantiomers. The 1′,8′-diazafluorenylidene units of two molecules A and B forming such a pair are parallel to each other and lie in a plane that makes a dihedral angle of 16° with the *xy* plane of the unit cell. The distance between the planes of the five-membered rings of each 1′,8′-fluorenylidene unit is 377.8.0 pm, and the torsion angle C^9(mol1)–$C^{9'}$(mol1)–$C^{9'}$(mol2)–C^9(mol2) is 180°.

NMR Spectroscopy

Table 2 gives the ^{1}H NMR chemical shifts of **6**–**8** and related homomerous BAEs. Table 3 gives the ^{13}C NMR chemical shifts of **6**–**8** and related BAEs. It is possible to distinguish qualitatively among the twisted conformation, the *anti*-folded conformation and the *syn*-folded conformation of a BAE in solution, using chemical shifts of the *fjord* protons H^1, H^8, $H^{1'}$, and $H^{8'}$. The *fjord* region protons of **6** appear at 8.33 (H^1, anthracenylidene moiety) and 7.74 ppm ($H^{1'}$, fluorenylidene moiety). These values differ from the chemical shifts of twisted **1** (δ = 8.39 ppm) and of *anti*-folded **2** (δ = 7.06 ppm). The UV/Vis spectra shows the presence of twisted conformation (absorption at 546 nm), but the observed H^1 and $H^{1'}$ chemical shifts are not suffi-

Table 1. Selected geometrical parameters of BAEs **2**, **5**–**8** derived from their crystal structures.

	ω twist deg	C^{9a}–C^{9}-$C^{9'}$–$C^{9a'}$ deg	C^{1}–C^{9}-$C^{9'}$–$C^{1'}$ deg	χ (C^{9}) deg	χ (C^{10}) deg	A–B C–D deg[c]	AEB–CFD deg[c]	C^{9}=$C^{9'}$ pm	$C^{10'}$–$O^{11'}$ pm	$C^{1}\cdots C^{1'}$ $N^{1}\cdots C^{1'}$ pm	$C^{8}\cdots C^{8'}$ $N^{8}\cdots C^{8'}$ pm	$H^{1}\cdots H^{1'}$ $N^{1}\cdots N^{1'}$ pm	$H^{8}\cdots H^{8'}$ $N^{8}\cdots N^{8'}$ pm	$C^{1}\cdots H^{1'}$ $N^{1}\cdots H^{1'}$ pm	$C^{8}\cdots H^{8'}$ $N^{8}\cdots H^{8'}$ pm
2[a]	0.0	3.6	35.0	3.6		40.0		136.4		294	294	304	304	281	281
		–3.6	–35.0	–3.6											
5[b]	42.3	43.3		0.6	–	0.5		140.1	–	312.5	314.4	244	242	273	272
		41.4		–1.3	–	1.4								258	254
6	3.2	7.2	–19.8	0.4	–	11.8	43.4	136.3	–	301.7	309.1	255.3	234.4	288.8	283.0
	0.0	–0.9	27.4	–8.5	7.8	51.1	0.0		122.2					240.4	239.3
7	3.2	–2.0	27.1	3.0	–	15.8	32.6	137.4	–	293.2	302.3	250.1	232.1	236.7	240.1
	0.0	8.4	–20.3	7.4	5.9	43.3	0.0		122.9					277.1	269.5
8	3.5	4.7	–17.2	4.9	–	7.5	43.8	136.3	–	278.1	286.9	–	–	261.6	252.6
	0.0	2.2	25.9	–7.4	6.8	47.5	0.0		122.2						

[a] Ref.[29] [b] Ref.[5] [c] See Figure 1.

Table 2. ^{1}H NMR chemical shifts (ppm) of **6**–**8** and related BAEs.

	Y	X	H^{1}, H^{8} $H^{1'}$, $H^{8'}$	H^{2}, H^{7} $H^{2'}$, $H^{7'}$	H^{3}, H^{6} $H^{3'}$, $H^{6'}$	H^{4}, H^{5} $H^{4'}$, $H^{5'}$
1	–	–	8.386	7.211	7.332	7.709
2	CO	CO	7.062	7.148	7.400	8.093
6	CO	–	8.331	7.448	7.497	8.235
			7.735	7.003	7.273	7.642
7	CO	–	8.442			8.275
			7.825, 8.264[a]			7.751[b], 8.025
8	CO	–	8.607	7.511	7.511	8.090
				8.341	7.194	7.900
17[c]	–	–	9.001	7.212	7.342	7.587
				8.626	7.258	8.003

[a] $H^{10'}$. [b] $H^{4'}$ or $H^{6'}$. [c] Ref.[17]

ciently shifted downfield as it would be expected for a twisted conformation. Evidently, there are fast interconversions of the twisted **t-6** and the *anti*-folded **a-6** conformers in solution. The observed chemical shifts of **6** are the averaged shifts of its two conformers. In **7**, the most downfield fluorylidene proton appears at δ = 8.26 ppm, indicating that also in this case the twisted **t-7** and the *anti*-folded **a-7** conformers interconvert rapidly in solution on the NMR timescale. In the case of **8**, the *fjord* region protons H^1 and H^8 appear at δ = 8.61 ppm, which may suggest that **8** adopts only a twisted conformation in solution. The dark red color of **8** in solution (longest wavelength absorption at 525 nm) also corresponds to a twisted conformation. However, the downfield shift of the *fjord* region protons H^1 and H^8 can also be explained by the effect of the *fjord* nitrogens at positions 1′ and 8′. The H^1 *fjord* protons in diaza-substituted **8** are shifted downfield relatively to H^1 and $H^{1'}$ of the parent **6** by 0.28 and 0.87 ppm. The latter value is characteristic for twisted conformations, where the *fjord* protons are bucking towards the *fjord* nitrogens, whereas the former value corresponds to an *anti*-folded conformation.[17] We conclude, that BAEs **6**–**8** demonstrate an equilibrium between a twisted conformation and a *anti*-folded conformation in solution at room temperature.

Dynamic Stereochemistry

The BAEs undergo the following three fundamental dynamic processes:[1c]

(a) *E*,*Z*-isomerization or *E*,*Z*-topomerization (Figure 5).
(b) Conformational inversion, i.e. inversion of the helicity in twisted BAEs or inversion of the boat conformations in the central rings of *anti*-folded BAEs (Figure 6).
(c) *syn*,*anti* isomerization (Figure 7).

Enantiomerization and conformational inversion may be considered in all three processes.

In the present study, only the *E*,*Z*-topomerization of **7** has been revealed, using dynamic NMR spectroscopy. The ^{1}H NMR spectrum of **7** at 297 K (in CD_2Cl_2) included one very broad signal centered at δ = 8.37 ppm, amounting to two protons, H^1 and H^8 of the anthracenylidene moiety. However, in the ^{1}H NMR spectrum of **7** recorded at 317 K, a doublet at δ = 8.45 ppm replaced the broad signal, whereas the spectrum recorded at 268 K revealed two doublets at δ = 8.30 and 8.48 ppm, clearly indicating a dynamic process. Both conformational inversion and *syn*, *anti* isomerization involve two parallel pathways with double barriers of equal heights. Inversion of helicity *P*/*M* of the central double bond through an *anti*-folded intermediate or *syn*-folded conformer would result in two complete sets of aromatic protons appearing in the ^{1}H NMR spectrum of **7** at low temperature. Topomerization, on the other hand, is a one step process of rotating along the central double bond, through an almost orthogonally twisted transition state. In this case, only the *fjord* region protons of the anthrone moiety are expected to demonstrate a difference in their chemical shifts, which agrees with the observations. The mechanism of *E*,*Z*-topomerization of twisted BAE **7** is depicted

Table 3. ^{13}C NMR chemical shifts (ppm) of **6**–**8** and related BAEs.

	Y	X	C^1, C^8 $C^{1'}$, $C^{8'}$	C^2, C^7 $C^{2'}$, $C^{7'}$	C^3, C^6 $C^{3'}$, $C^{6'}$	C^4, C^5 $C^{4'}$, $C^{5'}$	C^{4a}, C^{10a} $C^{4a'}$, $C^{4b'}$	C^{8a}, C^{9a} $C^{8a'}$, $C^{9a'}$	C^9 $C^{9'}$	C^{10}
1	–	–	126.73	126.85	129.15	119.89	141.31	138.28	141.01	
2	CO	CO	129.56	130.30	128.38	126.79	134.43	139.10	132.04	186.71
6	CO	–	130.74	130.61	128.89	127.20	132.95	138.40	134.14	185.24
			126.20	126.28	129.29	119.74	141.51	139.84	140.50	
8	CO	–	132.86	129.20	129.29	125.95	133.07	138.45	143.39	186.47
				147.53	122.83	126.88	131.32	156.58	132.65	
17[a]	–	–	130.57	127.07	130.97	119.24	142.94	148.71	148.71	
				148.11	122.41	127.28	131.65	136.01	136.01	

[a] Ref.[17]

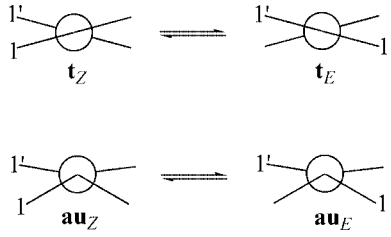

Figure 5. *E*,*Z*-Isomerization of BAEs.

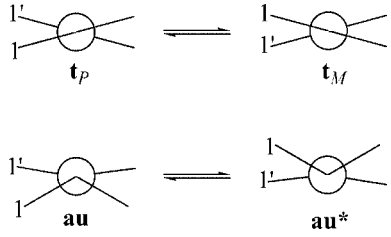

Figure 6. Conformation inversion of twisted and *anti*-folded BAEs.

Figure 7. The *syn*,*anti* isomerization of BAEs.

in Figure 8. A dynamic NMR spectroscopic study of **7** was performed at low temperatures. The thermal topomerization of **7** was studied by monitoring the coalescence of the two lowest field doublets of the anthracenylidene protons H^1 and H^8. The coalescence point was reached at 297 K (the extrapolated frequency difference $\Delta\nu_c$ is 51.7 Hz), which corresponds to the topomerization barrier of 63.4 kJ/mol. The rate of passing through one of the two alternative transition states, depicted in Figure 8, is half of the effective rate for topomerization, hence the total barrier height is $\Delta G_c^{\ddagger}(\mathbf{t}_\perp) = \Delta G_c^{\ddagger} + \boldsymbol{R}\cdot T\cdot\ln 2 = 65.5$ kJ/mol (at 297 K in CD_2Cl_2). For comparison, the *E*,*Z*-isomerization barriers of 2,2′-disubstituted bianthrones lie in the range 83.7–90.0 kJ/mol.[30] In fluorenylidenexanthene (**5**), the *E*,*Z*-isomerization barrier is 82.0 kJ/mol.[15]

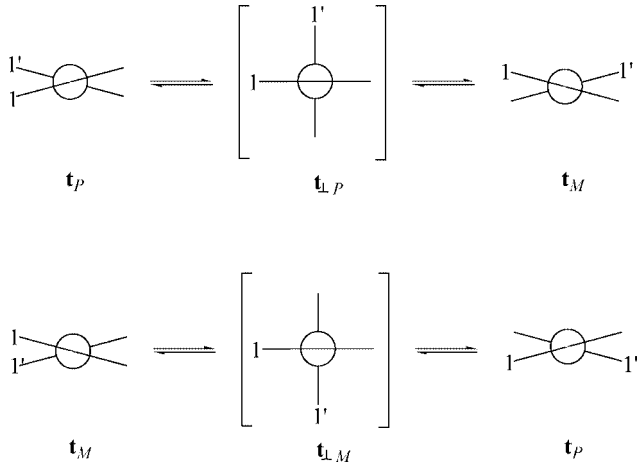

Figure 8. Schematic mechanism of the topomerization of **7**.

DFT Study

DFT methods are capable of generating a variety of isolated molecular properties quite accurately, especially via the hybrid functionals, and in a cost-effective way.[31] Recently, the B3LYP hybrid functional was successfully employed to treat overcrowded BAEs.[14,32] Bifluorenylidene (**1**), bianthrone (**2**), fluorenylidene-anthrone (**6**), and their 1,8-diaza and 1,8,1′,8′-tetraaza derivatives 9-(9′*H*-fluoren-9′-ylidene)-1,8-diaza-9*H*-fluorene (**17**), 9-(1′,8′-diaza-9′*H*-fluoren-9′-ylidene)-1,8-diaza-9*H*-fluorene (**18**), 10-[10′-oxo-9′(10′*H*)-anthracenylidene]-1,8-diaza-9(10*H*)-anthracenone (**19**), 10-[1′,8′-diaza-10′-oxo-9′(10′*H*)-anthracenylidene]-1,8-diaza-9(10*H*)-anthracenone (**20**), 1′,8′-diazafluorenylidene-anthrone (**8**), 10-(9′*H*-fluoren-9′-ylidene)-1,8-diaza-9(10*H*)-anthracenone (**21**), 10-(1′,8′-diaza-9′*H*-fluoren-9′-ylidene)-1,8-diaza-9(10*H*)-anthracenone (**22**) were chosen for a systematic computational DFT study of the effect of introducing nitrogen atoms at the *fjord* regions of BAEs on their thermochromism. The relative energies of these BAEs are presented in Table 4. Selected geometrical parameters of BAEs under study are presented in Table 5. The following analysis is based on the DFT enthalpies ΔH_{298} calculated from B3LYP/6-311++G(d,p) energies and thermal corrections to enthalpy computed at B3LYP/6-31(d) or B3LYP/6-311(d,p) (vide infra).

Table 4. The DFT relative energies (kJ/mol) of BAEs **1**, **2**, **6**–**8**, **17**–**22**.

			B3LYP/6-31G(d)				B3LYP/6-311G(d,p)			B3LYP/6-311++G(d,p)	
			[a]	ΔE_{Tot}	ΔH_{298}	ΔG_{298}	[a]	ΔE_{Tot}	ΔH_{298}[b]	ΔE_{Tot}	ΔH_{298}[b]
2	**t**	D_2	M	12.04	11.54	12.11	M	17.16	16.73[c]	19.11	18.67[c]
	a	C_{2h}	M	0.00	0.00	0.00		0.00	0.00	0.00	0.00
19	**t**	C_2	M	–3.02	–3.17	–2.12		1.23	1.09	4.01	3.86
	a	C_s	M	0.00	0.00	0.00		0.00	0.00	0.00	0.00
20	**t**	D_2	M	–1.89	–2.76	–1.40		0.86	0.004	5.39	4.53
	a	C_{2h}	M	0.00	0.00	0.00		0.00	0.000	0.00	0.00
6	**t**	C_2	M	0.00	0.00	0.00		0.00	0.00	0.00	0.00
	a	C_s	M	5.37	5.71	3.70	M	1.90	2.20[c]	0.47	0.78[c]
7	**t**	C_1	M	0.00	0.00	0.00		0.00	0.00	0.00	0.00
	a	C_1	M	5.54	5.91	5.88		1.93	2.29	0.92	1.28
8	**t**	C_2	M	7.45	7.67	9.91	M	11.20	11.37[c]	10.55	10.72[c]
	f	C_s	M	0.00	0.00	0.00		0.00	0.00	0.00	0.00
21	**t**	C_2	M	0.00	0.00	0.00		0.00	0.00	0.00	0.00
	s	C_s	TS	24.87	23.29	30.85		21.65	20.07	20.20	18.62
22	**t**	C_2	M	0.00	0.00	0.00		0.00	0.00	0.00	0.00
	a	C_s	M	9.06	9.42	6.53		7.27	7.63	5.46	5.82
1	**t**	D_2	M	0.00	0.00	0.00		0.00	0.00	0.00	0.00
	a	C_{2h}	M	38.90	39.62	37.17		36.40	37.12	36.19	36.90
17	**t**	C_2	M	0.00	0.00	0.00		0.00	0.00	0.00	0.00
	s	C_s	TS	16.72	14.58	19.55		14.85	12.71	17.07	17.94
18	**t**	D_2	M	0.00	0.00	0.00		0.00	0.00	0.00	0.00
	a	C_{2h}	TS	25.52	22.44	26.80		25.04	21.95	26.39	23.30

[a] M = minimum, TS = transition state. [b] The thermal correction to enthalpy was computed at B3LYP/6-31G(d) unless specified otherwise. [c] The thermal correction to enthalpy was computed at B3LYP/6-311G(d,p).

Bifluorenylidene (**1**), a Type 3 BAE, adopts twisted conformation **t-1** (pure twist 34.0°) as the global minimum. It has $C^1\cdots H^{1'}$ contact distance of 259.9 pm (penetration of 9%). Its *anti*-folded conformation **a-1** (folding 24.3°) is less stable than **t-1** by 36.9 kJ/mol and significantly more overcrowded, with $C^1\cdots C^{1'}$ and $C^1\cdots H^{1'}$ distances of 306.0 pm (penetration of 11%) and 243.8 pm (penetration of 15%), respectively.

Introduction of two nitrogen atoms into 1 and 8 positions of **1** does not relieve **17** of overcrowding but enhances it: the $N^1\cdots H^{1'}$ contact distance reaches 222.5 pm (15% penetration) in the twisted **t-17** and 206.6 ppm (22% penetration) in the folded **s-17**. It is accompanied by decrease of pure twist in **t-17** (28.0°) and folding in **s-17** (5.7° and 17.4°). Unlike the *anti*-folded **a-1**, the folded conformation of **17** is *syn*-folded (characterized by very small C^{8a}–C^9–$C^{9'}$–$C^{8a'}$ angle, ±0.4° vs. ±9.6° in **a-1**, smaller N^1–C^9–$C^{9'}$–$C^{1'}$ angle than in **a-1**, ±3.6° vs. ±14.6°, and large bistricyclic dihedral, 30.2° vs. 0°). It is not a minimum, but a transition state for the enantiomerization of **t-17**. No *anti*-folded conformation was found in the conformational space of **17**. The *syn*-folded **s-17** conformation, despite its being a transition state, is closer in enthalpy to the twisted **t-17** conformation (ΔH_{298} = 17.9 kJ/mol) than the *anti*-folded **a-1** to the twisted **t-1** (ΔH_{298} = 36.9 kJ/mol). The folded **a-18** conformation of tetraaza-substituted **18** is also a transition state and is higher in enthalpy than twisted **t-18** by 23.3 kJ/mol, which is more than in **s-17** but less than in **a-1**. It is *anti*-folded (the torsion angles C^{8a}–C^9–$C^{9'}$–$C^{8a'}$ and N^1–C^9–$C^{9'}$–$N^{1'}$ are ±7.3° and ±12.3°, respectively) and has a folding of 17.7°, larger than in diaza-substituted tricyclic moiety of **s-17**. The twisted conformation **t-18** also has larger pure twist (31.0°) than **t-17**. The folded **a-18** conformation has the N^1–$N^{1'}$ distance of 276.7 pm (8% penetration), while **t-18** is almost not overcrowded.

Thermochromic bianthrone (**2**) adopts *anti*-folded conformation **a-2** as its global minimum, with a folding of 42.7°. It is overcrowded, with $C^1\cdots C^{1'}$ distance of 303.1 pm (12% penetration). Its twisted conformation **t-2** lies 18.7 kJ/mol at B3LYP/6-311++G(d,p) and 16.7 kJ/mol at B3LYP/6-311G(d,p) higher than **a-2**. It has a pure twist of 55.4°, a folding of 5.0°, and is also overcrowded, with $C^1\cdots C^{1'}$ distance of 314.0 pm (penetration of 8%). The reported experimental enthalpy values ΔH_{A-B} are 11.3,[12e] 12.6 ± 0.8,[12f] 13.0,[12a] 13.8,[12a] 14.2,[12b,12d] 14.6 ± 2.5,[12c] 15.5,[12g] and 16.3.[12a] This newly calculated ΔH_{A-B} value is higher than that reported previously [ΔE = 12.0 kJ/mol at B3LYP/6-31G(d)].[14]

Introduction of two nitrogen atoms into the 1 and 8 positions of **2** lowers significantly the relative enthalpy of the twisted conformation **t-19**, by 14.8 kJ/mol. In this case the thermochromic conformation **t-19** is only 3.9 kJ/mol less stable than the *anti*-folded **a-19** conformation. Both **a-19** and **t-19** are slightly less overcrowded: the $N^1\cdots C^{1'}$ distances are 289.3 pm (10% penetration) and 297.0 pm (7% penetration). The relieve of steric strain is also expressed in smaller folding of the diaza-substituted tricyclic moieties of **a-19** (36.3°) and **t-19** (1.2°), as well as in smaller pure twist of **t-19** (53.5°). Introducing two additional nitrogen atoms into **19** slightly destabilizes the twisted conformation **t-20**, which is less stable than **a-20** by 4.5 kJ/mol. The twisted **t-20** (pure twist 50.0°) and the *anti*-folded **a-20** (folding 38.2°) conformations are both moderately overcrowded.

Fluorenylidene-anthrone (**6**) is a Type 3 BAE and has a twisted global minimum **t-6** conformation (pure twist 44.5°). However, its *anti*-folded **a-6** conformation is only

Table 5. Conformations and selected geometrical parameters of **1**, **2**, **6**–**8**, **17**–**22** derived from their crystal structures and DFT calculations [at B3LYP/6-311++G(d,p)].

			ω	C^{9a}–C^{9}–$C^{9'}$–C^{9a}	C^{1}–C^{9}–$C^{9'}$–$C^{1'}$	χ	χ	A–B	AEB–CFD	C^{9}–$C^{9'}$	$C^{1}\cdots C^{1'}$	$N^{1}\cdots N^{1'}$
					N^{1}–C^{9}–$C^{9'}$–$N^{1'}$	(C^{9})	(C^{10})	C–D			$N^{1}\cdots C^{1'}$	
			deg	deg	deg	deg	deg	deg[a]	deg[a]	pm	pm	pm
2	**t**	D_2	55.4	–55.4	–64.4	0.0	0.0	5.0	61.3	142.4	314.0	–
				–55.4	–64.4							
	a	C_{2h}	0.0	4.1	–36.4	–4.1	–8.1	42.7	0.0	136.5	303.1	–
				–4.1	36.4	–4.1	–8.1					
19	**t**	C_2	53.5	–53.5	–61.3	0.0	0.0	1.2	59.3	142.1	297.0	–
				–53.5	–61.3	0.0	0.0	5.4				
	a	C_s	0.0	2.6	–36.2	1.7	7.1	36.3	6.2	136.5	289.3	–
				–2.6	36.2	3.5	8.9	44.8				
20	**t**	D_2	50.0	–50.0	–58.9	0.0	0.0	4.7	55.9	140.4	–	281.7
				–50.0	–58.9	0.0	0.0					
	a	C_{2h}	0.0	2.5	–36.6	–2.5	–7.9	38.2	0.0	135.9	–	279.0
				–2.5	36.6	–2.5	–7.9					
6	**t**	C_2	44.5	–44.5	–53.4	0.0	–	4.6	52.3	139.8	313.4	–
				–44.5	–53.4	0.0	0.0	7.0				
	a	C_s	0.0	5.1	–25.2	4.1	–	17.3	33.3	136.6	303.8	–
				–5.1	25.2	6.2	9.3	47.8				
	X		3.2	7.2	–19.8	0.4	–	11.8	43.4	136.3	301.7	–
				–0.9	27.4	–8.5	7.8	51.1			309.1	
7	**t**	C_1	44.8	–44.8	–53.3	–0.1	–	4.0	52.2	140.0	312.5	–
				–44.7	–53.8	0.2	0.2	7.1			314.2	
	a	C_1	0.0	5.2	–25.4	–3.9	–	18.0	32.5	136.7	303.8	–
				–5.2	25.5	–6.5	–9.3	48.2			304.3	
	X		3.2	8.4	–20.3	3.0	–	15.8	32.6	137.4	293.2	–
				–2.0	27.1	7.4	5.9	43.3			302.3	
8	**t**	C_2	42.6	–42.6	–50.3	0.0	–	4.7	49.3	139.6	296.4	–
				–42.6	–50.3	0.0	0.0	7.2				
	f	C_s	0.0	1.7	–20.5	–11.8	–	2.7	52.7	137.2	280.4	–
				–1.7	20.5	8.3	8.6	45.3				
	X		3.5	4.7	–17.2	4.9	–	7.5	43.8	136.3	278.1	–
				2.2	25.9	–7.4	6.8	47.5			286.9	
21	**t**	C_2	41.4	–41.4	–48.5	0.0	–	4.5	49.1	139.7	293.7	–
				–41.4	–48.5	0.0	0.0	1.4				
	s	C_s	0.0	2.8	–15.9	–19.3	–	12.0	69.4	137.3	293.6	–
				–2.8	15.9	13.7	9.0	44.4				
22	**t**	C_2	40.6	–40.6	–49.0	0.0	–	3.5	47.6	138.4	–	284.3
				–40.6	–49.0	0.0	0.0	6.4				
	a	C_s	0.0	3.8	–24.3	–0.4	–	13.2	38.8	136.0	–	279.5
				–3.8	24.3	8.0	–8.3	41.6				
1	**t**	D_2	34.0	–34.0	–42.0	0.0	–	2.6	42.7	137.8	321.2	
				–34.0	–42.0	0.0						
	a	C_{2h}	0.0	9.6	–14.6	–9.6	–	24.3	0.0	137.1	306.0	
				–9.6	14.6	–9.6						
17	**t**	C_2	28.0	–28.0	–33.4	0.0	–	3.6	35.0	138.0	297.7	
				–28.0	–33.4	0.0	–	3.2				
	s	C_s	0.0	0.4	–3.6	12.2	–	5.7	30.2	138.6	284.4	
				–0.4	3.6	–12.9	–	17.4				
18	**t**	D_2	31.1	–31.0	–38.0	0.0	–	1.9	38.4	136.7	–	293.7
				–31.0	–38.0	0.0						
	a	C_{2h}	0.0	7.3	–12.3	–7.3	–	17.7	0.0	136.7	–	276.7
				–7.3	12.3	–7.3						

[a] See Figure 1.

0.78 kJ/mol higher than the twisted **t-6**. This difference between the conformations is translated into ca. 42% of **t-6** at equilibrium at room temperature. Therefore, BAE **6** should readily demonstrate solvatochromic behavior, acquiring in solution a deep color, which corresponds to the twisted **t-6** conformation. Indeed, **6** is yellow in the solid state and purple in solution. The ^{1}H and ^{13}C NMR spectra of **6**, however, show only one set of signals, evidently due to the fast interconversion of the twisted **t-6** and the *anti*-folded **a-6** diastereomers in solution (vide supra). The folding of the anthracenylidene moiety of **a-6** (48.4°) is much larger than the folding of the fluorenylidene moiety (17.3°). The respective values for **t-6** are 4.6° and 7.0°. The *anti*-folded **a-6** conformation, in spite of being close in energy to the twisted **t-6** conformation, is significantly overcrowded: the $C^{1}\cdots C^{1'}$ and $C^{1}\cdots H^{1'}$ distances are 303.8 pm (penetration of

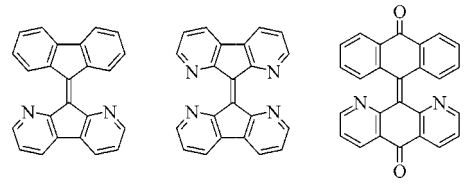

17 18 19

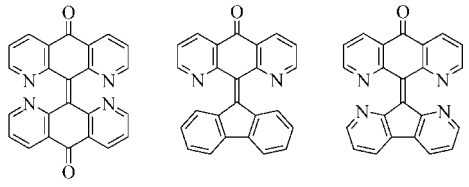

20 21 22

11%) and 242.9 pm (penetration of 15%), respectively. The respective values in **t-6** are 313.4 and 271.4 pm. The molecular structure of **6** as determined by X-ray crystallography corresponds to the calculated *anti*-folded **a-6** conformation. In general, there is good agreement between these two structures. The X-ray molecular structure does not possess C_s symmetry and has a small pure twist (3.2°) contrary to **a-6**, less folded fluorenylidene moiety (11.8° vs. 17.3°) and slightly more folded anthracenylidene moiety (51.1° vs. 48.4°). The degree of overcrowding is very similar in both structures. The only substantial difference between the experimental and the calculated structures of **6** is the bistricyclic dihedral, 43.4° vs. 33.3°. Linear benzannelation of **6** does not noticeably affect the energy difference between the *anti*-folded and the twisted conformations of **7**, which is 1.3 kJ/mol. The calculated geometries of **t-7** and **a-7** are also almost identical to the respective geometries of **6** (Table 5). The X-ray molecular structure of **7** is in the very good agreement with the calculated *anti*-folded **a-7** conformation. The latter predicts slightly larger folding of both fluorenylidene moiety (18.0° vs. 15.8°) and anthracenylidene moiety (48.2° vs. 43.3°) than the X-ray structure.

Two nitrogen atoms may be introduced in fluorenylideneanthrone (**6**) either at the fluorenylidene or at the anthracenylidene moiety, giving BAE **8** or BAE **21**, respectively. Fluorenylidene-1,8-diazaanthrone (**21**) adopts a twisted conformation **t-21** as the global minimum, with reduced a pure twist (41.4°) and a folding (1.4°) of the diaza-substituted anthracenylidene moiety. The folded **s-21** conformation is *syn*-folded (characterized by smaller C^{8a}–C^9–$C^{9'}$–$C^{8a'}$ angle, ±2.8° vs. ±5.2° in **a-7**, smaller than in **a-7** N^1–C^9–$C^{9'}$–$C^{1'}$ angle, ±15.9° vs. ±25.4°, and large bistricyclic dihedral, 69.4° vs. 32.5°). It is a transition state, higher in energy than **t-21** by 18.6 kJ/mol. The **s-21** conformation also has very short $N^1\cdots H^{1'}$ distance, 209.2 pm (21% penetration). No *anti*-folded conformation was found in the conformational space of **21**. By contrast, 1′,8′-diazafluorenylidene-anthrone (**8**) adopts a global minimum folded **f-8** conformation, which is more stable than the twisted **t-8** conformation (pure twist 42.6°) by 10.7 kJ/mol, which corresponds to merely 1.4% of **t-8** at equilibrium at 298 K. Obviously, the DFT calculations somewhat underestimate the stability of the twisted **t-8** conformation. Note also that **t-8** is more stable than its isomer **t-21** by 10.4 kJ/mol. The folded **f-8** conformation cannot be unambiguously defined as either *anti*-folded or *syn*-folded. Its fluorenylidene moiety is nearly planar (folding 2.7°). It has small C^{8a}–C^9–$C^{9'}$–$C^{8a'}$ angle (±1.7), medium C^1–C^9–$C^{9'}$–$N^{1'}$ angle (±20.5), large bistricyclic dihedral (52.7°). It also has a short $C^1\cdots N^{1'}$ distance (280.4 pm, 13% penetration) and nearly normal $H^1\cdots N^{1'}$ distance (253.7 pm, 4% penetration). The X-ray molecular structure of **8** is in a good agreement with calculated folded **f-8** conformation. The X-ray structure of **8** is slightly more folded (7.5° vs. 2.7° for the diazafluorenylidene moiety and 47.5° vs. 45.3° for the anthracenylidene moiety) and more twisted (3.5°) than calculated **f-8**. Contrary to **f-8**, the X-ray structure of **8** is clearly *syn*-folded. The bistricyclic dihedral in the X-ray structure of **8** is smaller (43.8° vs. 52.7°), than in **f-8**. Both the conformations have a similar degree of overcrowding.

Tetraaza-substituted heteromerous BAE **22** has a twisted global minimum **t-22** conformation (pure twist 40.6°). The *anti*-folded **a-22** conformation is less stable than **t-22** by 5.8 kJ/mol. It is less folded in the anthracenylidene unit (41.6°) than **s-21** (44.4°), but more folded in the fluorenylidene unit (13.2°) than **f-8** (2.7°). Both **t-22** and **a-22** are moderately overcrowded.

Thus, the introduction of nitrogen atoms into the *fjord* regions of BAEs affects dramatically the relative stabilities of their folded and twisted conformations. It is known, that the fluorenylidene moiety has an energetic propensity against folding, contrary to the anthracenylidene moiety, where folding is the preferred way to relieve the steric strain.[1c] The presence of nitrogen atoms in 1 and 8 positions of fluorenylidene unit destabilizes the twisted conformations, raising their energies relatively to the respective folded conformations by 11.5 (**8**), 13.6 (**18**), and 22.0 (**17**) kJ/mol. On the other hand, introduction of nitrogen atoms at the 1 and 8 positions of anthracenylidene unit destabilizes the folded conformations, raising their energies relatively to the twisted conformations by 14.8 (**19**), 14.1 (**20**), and 17.9 (**21**) kJ/mol. In the case of heteromerous BAE **22**, these effects work in the opposite directions, resulting in the small relative destabilization of the *anti*-folded a-22 conformation by 5.0 kJ/mol.

The effect of introducing of nitrogen atoms into the *fjord* regions of BAEs **1**, **2**, and **6** upon their relative stabilities can also be described by a series of homodesmic reactions[33] (Schemes 5 and 6). Combining a 1,8-diaza-substituted fluorenylidene unit with another fluorenylidene unit (**t-17**) appears to be preferable than combining it with an anthracenylidene unit (**f-8**): reaction (2) is exothermic (–16.3 kJ/mol), while reaction (1) is slightly endothermic (2.4 kJ/mol). Similarly, combining a 1,8-diaza-substituted anthracenylidene unit with a fluorenylidene unit (**f-21**) is preferable than combining it with an anthracenylidene unit (**a-19**), based on the endothermicities of the reactions (3) and (4), 20.2 and 1.6 kJ/mol, respectively. Reactions (5) and (6) demonstrate that the twisted 1,8,1′,8′-tetraaza-substi-

tuted bifluorenylidene derivative **t-18** is destabilized relative to two molecules of 1,8-diaza-substituted **t-17** by 34.5 kJ/mol, whereas the folded 1,8,1′,8′-tetraaza-substituted **a-20** is stabilized relative to two molecules of **a-19** by 15.3 kJ/mol. Reaction (7), which compares **t-18** and **a-20**, indicates a relative stabilization of folded **a-20** by 14.0 kJ/mol. Thus, tetraazasubstitution in the *fjord* regions promotes folding and impairs twisting in BAEs.

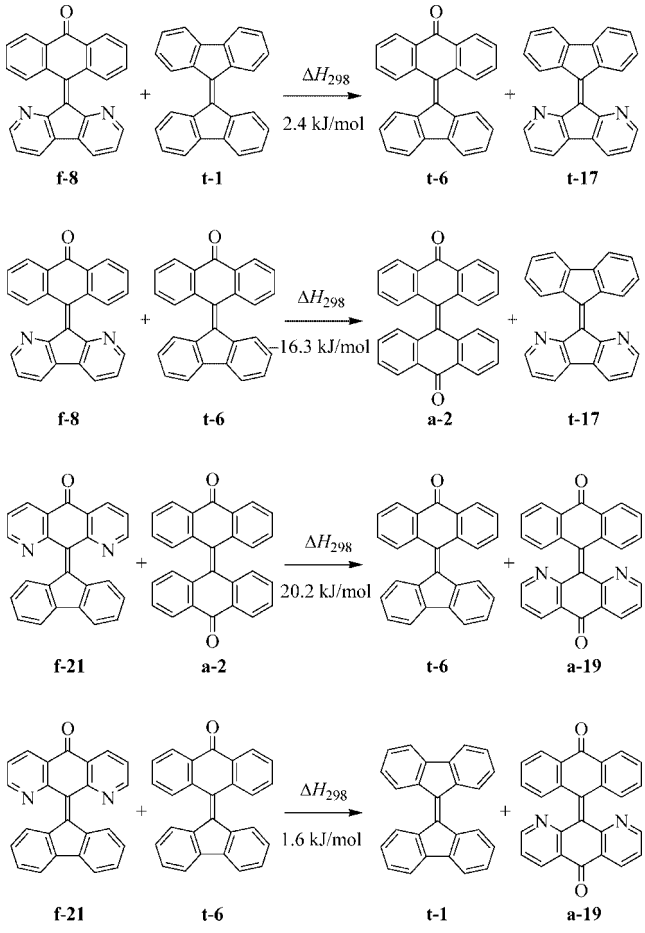

Scheme 5.

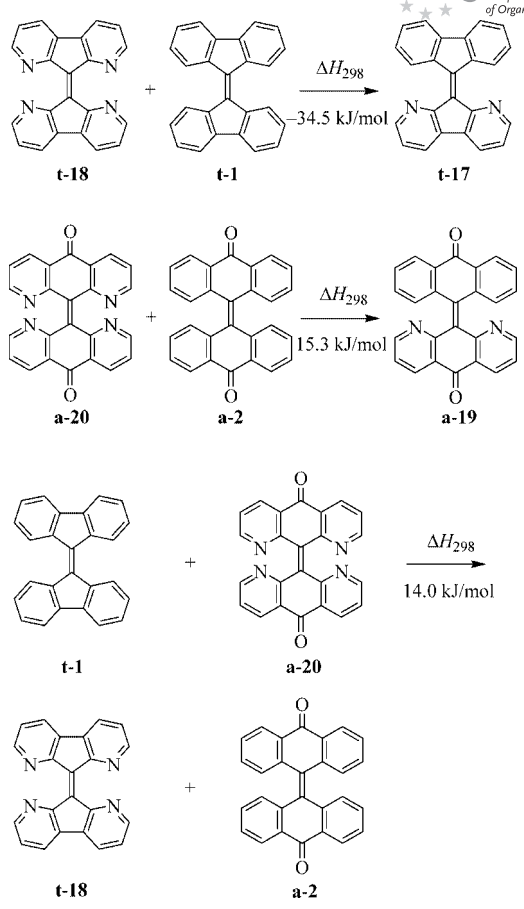

Scheme 6.

The basis set dependence of the relative stabilities of *anti*-folded and twisted conformations of the BAEs under study deserves a comment. The minimal basis set (Table S1) causes the twisted conformations to have the highest energies relative to the corresponding *anti*-folded conformations. Double split-valence basis set (Table 1) considerably stabilizes the twisted conformations, which become the global minima except in BAEs **2** and **8**. The further expansion of basis set up to diffuse functions augmented triple split-valence basis set moderately decreases the relative stabilities of the twisted conformations. In the cases of **19** and **20** it leads to the *anti*-folded conformations becoming global minima again.

The potential push-pull character of 1,8-diaza-substituted **6** and related BAEs can be analyzed by summing up the natural atomic charges of the atoms consisting each of the tricyclic moieties (Table S3). In the parent **6**, the anthracenylidene moiety bears negligibly small excess charges (–0.003 in **t-6** and 0.006 in **a-6**). 1,8-Diazasubstitution pulls the electron density into the fluorenylidene moiety of **8** (–0.180 in **t-8** and –0.132 in **f-8**) and into the anthracenylidene moiety of **t-21** (–0.210) and of **s-21** [–0.087 at B3LYP/6-311G(d,p); the high charge separation in **s-21** at B3LYP/6-31G++(d,p) is evidently an artefact of the diffuse function augmented basis set]. Two 1,8-diaza-substituted moieties in **22** mutually neutralize their effects; the small negative charges reside on the anthracenylidene half of **t-22** (–0.024) and of **a-22** (–0.021). Homomerous BAEs **17** and **19** also have excessive negative charge on their 1,8-diaza-substituted moieties: –0.225 in **t-17** and –0.143 in **s-17**, and –0.245 in **t-19** and –0.097 in **a-19**. With the exception of **22**, the zwitterionic character is enhanced in the twisted conformations due to the more planar tricyclic moieties.

Two somewhat bizarre reports on a thermochromism at room temperature deserve a comment. Bergmann wrote in 1948: "... dibiphenylethylene (i.e. **1**), which is intensely red, but loses its color when chilled to low temperature, the same phenomenon as in the case of dixanthylene may be assumed to occur, but in a different temperature range".[34] Ault, et al. reported in 1971: "Dixanthylene is a pale yellow-green solid at room temperature, but becomes dark blue when melted or heated in solution; at liquid nitrogen temperature,

it is completely colorless".[35] These observations at low temperatures have never been confirmed experimentally. Moreover, the computational results of the present study throw doubt on the presence of a colorless conformation of a Type 3 BAE **1**, (e.g. an *anti*-folded conformer) at "low temperature" and the presence of a colorless conformer of **3**, belonging to Type 1, at liquid nitrogen temperature, in addition to the *anti*-folded conformer found at room temperature.

Conclusions

BAEs **6**–**8** demonstrate a subtle equilibrium between the twisted and *anti*-folded conformations at room temperature. Their deep colors in solution indicate the presence of the readily populated the twisted conformations, while in the solid state these BAEs demonstrate yellowish colors of the *anti*-folded conformations. The twisted and *anti*-folded conformations interconvert rapidly on the NMR timescale. Introduction of the nitrogen atoms into the 1 and 8 positions of a fluorenylidene moiety affects the relative stability of the twisted and *anti*-folded conformations of BAEs, thus controlling their thermochromic behavior.

Experimental Section

Melting points are uncorrected. All NMR spectra were recorded with a Bruker DRX 400 spectrometer. ^{1}H NMR spectra were recorded at 400.1 MHz using $CDCl_3$ as solvent and as internal standard [δ($CHCl_3$) = 7.26 ppm]. The ^{1}H NMR of compound **7** was performed also at CD_2Cl_2 (δ = 5.31 ppm), and $C_2D_2Cl_4$ (δ = 5.99 ppm) at different temperatures. ^{13}C NMR spectra were recorded at 100.6 MHz using $CDCl_3$ as solvent and as internal standard [δ($CDCl_3$) = 77.0 ppm]. UV/Vis spectra were measured using an UVIKON 860 spectrometer. IR spectra were measured with a Perkin–Elmer System 2000 FT-IR spectrometer. Complete assignments were made through 2-dimentional correlation spectroscopy (DQF-COSY, HSQC, and HMBC). Petroleum ether (PE, boiling range 40–60 °C) was used. X-ray data were collected on a Bruker SMART APEX CCD diffractometer equipped with a graphite monochromator and using MoK_α radiation (λ = 0.71073 Å) (Table 6).

10-Diazo-9(10*H*)-anthracenone (12): Preparation according to the literature.[23,25] In a round-bottomed flask (250 mL) with reflux condenser and magnetic stirrer bar, *p*-toluenesulfonyl chloride (5.109 g, 26.8 mmol) was dissolved in ethanol (50 mL) under heating till everything was dissolved. Sodium azide (2.11 g, 32.5 mmol) was dissolved in water (6 mL) and was added to the flask. The reaction mixture was stirred at room temp. for 1–2 h. The precipitate of NaCl was filtered off. Anthrone (4.42 g, 22.7 mmol) was added and piperidine (2.5 mL) was added dropwise via syringe. The color of the reaction mixture turned red. The reaction mixture was stirred at room temp. for 5 h. The red precipitate was filtered off by using a Büchner funnel. Red crystals of **12** were obtained: 4.26 g, yield 72%. Recrystallization from 1,4- dioxane gave pure **12**, dec. 135–140 °C (ref.[23] dec. 150 °C). ^{1}H NMR ($CDCl_3$, 298 K): δ = 7.350 (ddd, ^3J = 8.1, ^4J = 1.1, ^5J = 0.6 Hz, 2 H), 7.411 (td, ^3J = 8.2, ^3J = 6.9, ^4J = 1.1 Hz, 2 H), 7.702 (td, ^3J = 8.1, 7.2, ^3J = 7.2, ^4J = 1.4 Hz, 2 H), 8.546 (ddd, ^3J = 8.0, ^4J = 1.4 Hz, ^5J = 0.6 Hz, 2 H) ppm. ^{13}C NMR ($CDCl_3$, 298 K): δ = 64.66 (C=N_2), 120.61 (C–H), 125.24 (C–H), 128.33 (C), 128.96 (C–H), 129.74 (C), 132.91 (C–H), 180.00 (C=O) ppm. IR (KBr): $\tilde{\nu}_{max}$ = 1630 (C=O), 2070 (N≡N) cm^{-1}.

10-Thioxo-9(10*H*)-anthracenone (10): Preparation according to the literature.[23] In a round-bottomed flask (25 mL) with reflux condenser and magnetic stirrer bar, diazo **12** (1 g, 4.5 mmol) was added with sulfur (0.172 g, 5.4 mmol) in DMF (10 mL) (dried before on Na_2SO_4 and distilled). The reaction mixture was heated in an oil bath (15 min) at 150–157 °C and evolution of N_2 was observed. The color of the reaction mixture turned from red to dark green. The flask was cooled down in an ice bath and the green precipitate was filtered off by using a Büchner funnel. The green crystals were washed with cold acetone and than dissolved in CH_2Cl_2, the solution was evaporated. A green powder of **10** was obtained: 0.434 g, yield of 43%, m.p. 208–210 °C (ref.[23] 213–214 °C). ^{1}H NMR ($CDCl_3$, 298 K): δ = 7.698 (td, 2 H), 7.817 (td, 2 H), 8.190 (ddd, 2 H), 8.547 (ddd, 2 H) ppm. ^{13}C NMR ($CDCl_3$, 298 K): δ = 126.42 (C–H), 127.91 (C), 130.07 (C–H), 133.43 (C–H), 133.48 (C–H), 138.13 (C), 185.00 (C=O), 218.59 (C=S) ppm.

Table 6. Crystallographic data for BAEs **6**–**8**.

	6	**7**	**8**
Empirical formula	$C_{27}H_{16}O$	$C_{31}H_{18}O$	$C_{25}H_{14}N_2O$
Temperature /K	295(1)	123(1)	295(1)
Crystal system	monoclinic	orthorhombic	monoclinic
Space group	$P2_1/n$	$Pbca$	$P2_1/n$
a /Å	13.2593(9)	8.262(5)	13.1607(8)
b /Å	9.7518(7)	21.77(1)	9.6404(6)
c /Å	14.189(1)	23.00(2)	14.1537(9)
α /deg	90.0	90.0	90.0
β /deg	107.568(1)	90.0	108.003(1)
γ /deg	90.0	90.0	90.0
V /Å^3	1749.1(2)	4136(5)	1707.8(2)
Z	4	8	4
Density (calcd.) /Mg/m^3	1.353	1.305	1.394
Reflections collected	18977	45271	18496
Independent reflections	3809	4964	3721
	[R(int) = 0.0328]	[R(int) = 0.2129]	[R(int) = 0.0248]
Final R indices [$I > 2\sigma_I$]	R_1 = 0.0424	R_1 = 0.0793	R_1 = 0.0421
	wR_2 = 0.1007	wR_2 = 0.1440	wR_2 = 0.1081

Dispiro[9*H*-fluorene-9,2′-thiirane-3′,9′′-(10′′*H*)antracenone] (13): To a stirred solution of diazo **9** (0.214 g, 1.11 mmol) in anhydrous CH_2Cl_2 (20 mL) under argon atmosphere, thione **10** (0.25 g, 1.11 mmol) was added via syringe. The reaction mixture was stirred at room temp. for 48 h. Trituration with ethanol gave a precipitate which was filtered off on a glass frit. A yellow power of **13** was obtained: 0.172 g in a yield 38%. ^{1}H NMR ($CDCl_3$, 298 K): δ = 6.808 (dt, ^3J = 8.3, ^3J = 7.8 Hz, 2 H), 6.903 (d, ^3J = 7.8 Hz, 2 H), 7.129 (dt, ^3J = 8.4, ^3J = 7.5 Hz, 2 H), 7.345 (dt, ^3J = 8.6, ^3J = 7.6 Hz, 2 H), 7.471 (d, ^3J = 7.6 Hz, 2 H), 7.585 (dt, ^3J = 8.9, ^3J = 7.6 Hz, 2 H), 7.764 (d, ^3J = 7.6 Hz, 2 H), 8.173 (d, ^3J = 7.6 Hz, 2 H) ppm. ^{13}C NMR ($CDCl_3$, 298 K): δ = 57.38 (C–S), 58.68 (C–S), 119.73 (C–H), 124.27 (C–H), 125.87 (C–H), 127.07 (C–H), 128.07 (C–H), 128.32 (C–H), 128.37 (C–H), 130.76 (C–H), 135.93 (C), 140.58 (C), 141.16 (C), 141.74 (C), 185.92 (C=O) ppm.

10-(9*H*-Fluoren-9′-ylidene)-9(10*H*)-anthracenone (6): I To a stirred solution of diazo **12** (0.809 g, 3.76 mmol) in anhydrous benzene (60 mL) and protected by a $CaCl_2$ tube, thione **11** (0.757 g, 3.86 mmol) was added. The reaction mixture was refluxed for 7 h. After cooling and standing for 48 h a precipitate was obtained which was filtered in a sinter fritte. A yellow power of **6** was obtained: 0.430 g, yield 33%, m.p. 279–281 °C (ref.[19] 280 °C dec.;[20] 283–284 °C).

II: To a stirred solution of diazo **9** (0.576 g, 2.57 mmol) in $CHCl_3$ dried on molecular sieves (4 Å, 35 mL) and protected by a $CaCl_2$ tube, thione **10** (0.493 g, 2.57 mmol) was added. The reaction mixture was refluxed overnight. The color of the reaction mixture was purple. The mixture was cooled to room temp., and the solvent was removed under reduced pressure. Trituration of the crude product in hot benzene gave a precipitate, which was filtered off. A yellow power 0.408 g of **6** was obtained, in a yield of 46%, m.p. 280–281 °C (ref.[19] 280 °C dec.;[20] 283–284 °C).

III: To a stirred solution of thiirane **13** (0.166 g, 0.427 mmol) in anhydrous dry benzene (15 mL) PPh_3 (0.567 g, 2.16 mmol) was added. The reaction was stirred overnight while reflux under protection of $CaCl_2$. After cooling the solvent was evaporated till dryness. A trituration in ethanol gave a precipitate which was filtered in a sinter fritte. A yellow power of **6** was obtained, 0.035 g in a yield 23%, m.p. 279–282 °C (ref.[19] 280 °C dec.;[20] 283–284 °C). A single crystal was obtained from NMR tube in $CDCl_3$.

^{1}H NMR ($CDCl_3$, 298 K): δ = 7.003 (td, J = 7.3 Hz, 2 H, H$^{2'}$, H$^{7'}$), 7.273 (td, J = 7.3 Hz, 2 H, H$^{3'}$, H$^{6'}$), 7.448 (td, J = 7.7 Hz, 2 H, H^2, H^7), 7.497 (td, J = 7.5 Hz, 2 H, H^3, H^6), 7.642 (ddd, J = 7.4 Hz, 2 H, H$^{4'}$, H$^{5'}$), 7.735 (ddd, J = 8.0 Hz, 2 H, H$^{1'}$, H$^{8'}$), 8.235 (ddd, J = 7.6 Hz, 2 H, H^4, H^5), 8.331 (ddd, J = 7.6 Hz, 2 H, H^1, H^8) ppm. ^{13}C NMR ($CDCl_3$, 298 K): δ = 119.74 (C$^{4'}$, C$^{5'}$), 126.20 (C$^{1'}$, C$^{8'}$), 126.28 (C$^{2'}$, C$^{7'}$), 127.20 (C^4, C^5), 128.89 (C^3, C^6), 129.29 (C$^{3'}$, C$^{6'}$), 130.61 (C^2, C^7), 130.74 (C^1, C^8), 132.95 (C^{4a}, C^{10a}), 134.14 (C^9), 138.40 (C^{8a}, C^{9a}), 139.84 (C$^{8a'}$, C$^{9a'}$), 140.50 (C$^{9'}$), 141.51 (C$^{4a'}$, C$^{4b'}$), 185.24 (C^{10}) ppm.

10-(11′*H*-Benzo[*b*]fluoren-11′-ylidene)-9(10*H*)-anthracenone (7): To a stirred solution of 9-diazobenzo[*b*]fluorenone[26] (**14**) (0.278 g, 1.14 mmol) in $CHCl_3$ (7 mL) and protected by a $CaCl_2$ tube, thione **10** (0.246 g, 1.14 mmol) dissolved in $CHCl_3$ (7 mL) was added via syringe. The reaction mixture was refluxed overnight. After cooling to room temp. the reaction mixture was evaporated on silica gel and purified by column chromatography on a dry silica gel (eluent PE/CH_2Cl_2, gradient 100–70% PE). The first fraction was identified as (*E*)- and (*Z*)-11-(11′*H*-benzo[*b*]fluorene-11′-ylidene)-11*H*-benzo[*b*]fluorene (0.040 g), the second fraction was identified as 9,10-anthraquinone (0.340 g), the third fraction was **7**. A second column chromatography at the same conditions afforded **7**: 0.060 g, yield 13% as a yellow green powder, m.p.172–176 °C. A single crystal was obtained from sublimation in a sealed tube under vacuum at 200 °C ^{1}H NMR ($CDCl_3$, 298 K): δ = 7.053 (td, 1 H), 7.312–7.378 (m, 2 H), 7.420–7.471 (m, 3 H), 7.496–7.549 (m, 3 H), 7.751 (d, 1 H, H$^{4'}$ or H$^{6'}$), 7.803–7.848 (m, 2 H, H$^{1'}$, H$^{4'}$ or H$^{6'}$), 8.025 (s, 1 H, H$^{5'}$), 8.264 (s, 1 H, H$^{10'}$), 8.275 (d, 2 H, H^4, H^5), 8.442 (br. s, 2 H, H^1, H^8) ppm. ^{13}C NMR ($CDCl_3$, 298 K): δ = 117.71 (C–H), 120.54 (C–H), 125.89 (C–H), 126.04 (C–H), 126.28 (C–H), 126.86 (C–H), 127.15 (C–H), 127.25 (C–H), 128.17 (C–H), 128.80 (C–H), 129.39 (C–H), 129.60 (C–H), 130.18, 130.55, 132.46, 132.76 (C), 132.93 (C–H), 133.98 (C), 134.12 (C), 138.29 (C), 138.54 (C), 138.68 (C), 140.38 (C), 141.37 (C), 141.49 (C), 185.18 (C^{10}) ppm. UV/Vis (cyclohexane): $c = 2.36 \times 10^{-5}$ M. λ_{max} nm (ε): 389 (11822), 590 (8771). ^{1}H NMR (CD_2Cl_2, 297 K): δ = 7.057 (td, 1 H), 7.321–7.379 (m, 2 H), 7.423–7.484 (m, 3 H), 7.484–7.552 (m, 3 H), 7.742 (d, 1 H), 7.826–7.857 (m, 2 H), 8.056 (s, 1 H, H$^{5'}$), 8.199 (d, 2 H, H^4, H^5), 8.259 (s, 1 H, H$^{10'}$), 8.367 (br. s, 2 H, H^1, H^8) ppm. ^{1}H NMR (CD_2Cl_2, 268 K): δ = 7.046 (td, 1 H), 7.313–7.372 (m, 2 H), 7.422–7.546 (m, 6 H), 7.730 (d, J = 8.0 Hz, 1 H), 7.805–7.849 (m, 2 H), 8.052 (s, 1 H, H$^{5'}$), 8.153 (d, J = 8.0 Hz, 1 H, H^4 or H^5), 8.190 (d, J = 8.0 Hz, 1 H, H^4 or H^5), 8.25 (s, 1 H, H$^{10'}$), 8.296 (d, J = 8.0 Hz, 1 H, H^1 or H^8), 8.478 (d, J = 7.9 Hz, 1 H, H^1 or H^8) ppm. ^{1}H NMR ($C_2D_2Cl_4$, 268 K): δ = 7.083 (td, 1 H), 7.267–7.3859 (m, 2 H), 7.424–7.587 (m, 6 H), 7.702 (d, J = 8.0 Hz, 1 H), 7.778–7.832 (m, 2 H), 8.062 (s, 1 H, H$^{5'}$), 8.202 (d, J = 8.0 Hz, 1 H, H^4 or H^5), 8.233 (d, J = 8.0 Hz, 1 H), 8.245 (s, 1 H, H$^{10'}$), 8.347 (d, J = 7.6 Hz, 1 H, H^1 or H^8), 8.518 (d, J = 8.0 Hz, 1 H, H^1 or H^8) ppm.

Dispiro[9*H*-1,8-diazafluorene-9,2′-thiirane-3′,9′′-(10′′*H*)-anthracenone] (16): To a stirred solution of diazo[17,27] **15** (0.262 g, 1.35 mmol) dissolved in CH_2Cl_2 (25 mL) under argon atmosphere, thione **10** (0.302 g, 1.35 mmol) was added via syringe. The reaction mixture was stirred overnight at room temp. The solvent was removed under reduced pressure. Trituration of the crude product in $CHCl_3$ gave a precipitate, which was filtered off. A grey power of **16** was obtained: 0.344 g, yield 71%, dec. 122–124 °C. ^{1}H NMR ($CDCl_3$, 298 K): δ = 7.041 (td, 2 H), 7.349 (td, 2 H), 7.594 (td, 2 H), 7.719 (dd, 2 H), 7.782 (dd, 2 H), 8.089 (dd, 2 H), 8.461 (dd, 2 H) ppm. ^{13}C NMR ($CDCl_3$, 298 K): δ = 55.03 (C–S), 57.50 (C–S), 122.68 (C–H), 125.97 (C–H), 127.51 (C–H), 128.05 (C–H), 130.22 (C–H), 131.39 (C–H), 133.21 (C), 135.03 (C), 137.87 (C), 147.47 (C–H), 159.51 (C), 186.06 (C^{10}) ppm.

10-(9*H*-1,8-Diazafluorene-9′-ylidene)-9(10*H*)-anthracenone (8): To a stirred solution of thiarane **16** (0.300 g, 0.769 mmol) in anhydrous benzene (20 mL) PPh_3 (0.503 g, 1.922 mmol) was added. The reaction was stirred 3 h while reflux under protection of $CaCl_2$. After cooling the solvent was evaporated till dryness.A trituration in ethanol gave a precipitate which was filtered in a sinter fritte. Purification was performed by column chromatography on silica gel while the compound was dissolved in CH_2Cl_2 and charged on the column using CH_2Cl_2/Et_3N (98:2) as eluent. The red fraction was collected and evaporated; 0.090 g of **8** was obtained as yellow powder, yield 33%, m.p. 147 °C. A single crystal of **8** was obtained from $CDCl_3$. ^{1}H NMR ($CDCl_3$, 298 K): δ = 7.194 (td, ^3J = 7.6, ^3J = 4.8 Hz, 2 H, H$^{3'}$, H$^{6'}$), 7.511 (m, 4 H, H^3, H^6, H^2, H^7), 7.900 (dd, ^3J = 7.6, ^4J = 1.5 Hz, 2 H, H$^{4'}$, H$^{5'}$), 8.090 (m, 2 H, H^4, H^5), 8.341 (ddd, ^3J = 4.8, ^4J = 1.4 Hz, 2 H, H$^{2'}$, H$^{7'}$), 8.607 (m, 2 H, H^1, H^8) ppm. ^{13}C NMR ($CDCl_3$, 298 K): δ = 122.83 (C$^{3'}$, C$^{6'}$), 125.95 (C^4, C^5), 126.88 (C$^{4'}$, C$^{5'}$), 129.20 (C^3, C^6 or C^2, C^7), 129.29 (C^2, C^7 or C^3, C^6), 131.32 (C$^{4a'}$, C$^{4b'}$), 132.65 (C$^{9'}$), 132.86 (C^1, C^8), 133.07 (C^{4a}, C^{10a}), 138.45 (C^{8a}, C^{9a}), 143.39 (C^9), 147.53 (C$^{2'}$, C$^{7'}$), 156.58 (C$^{8a'}$, C$^{9a'}$), 186.47 (C^{10}) ppm. UV/Vis (cyclohexane): $c = 2.77 \times 10^{-5}$ M,

λ_{max} nm (ε): 370 (10288); $c = 6.92 \times 10^{-4}$ M, λ_{max} nm (ε): 525 (sh, 739).

Computation Details: The quantum-mechanical calculations of the BAEs under study were performed using the Gaussian03[36] package. Becke's three-parameter hybrid density functional B3LYP,[37] with the non-local correlation functional of Lee, Yang, and Parr[38] was used. The basis sets STO-3G, 6-31G(d), 6-311G(d,p), and 6-311++G(d,p) were employed. All structures were fully optimized using symmetry constrains as indicated. Vibrational frequencies were calculated to verify the nature of the stationary points at B3LYP/6-31G(d) for all the BAEs and at B3LYP/6-311G(d,p) for BAEs **2**, **6**, and **8**. Non-scaled thermal corrections to enthalpy calculated at the specified levels were applied to the B3LYP/6-311++G(d,p) calculated energies to estimate the enthalpies ΔH_{298}. Comparison between the B3LYP/6-311G(d,p) values of ΔH_{298} to the estimated ones obtained from the B3LYP/6-311G(d,p) energies and the thermal corrections at B3LYP/6-31G(d) revealed very small differences of 0.04–0.07 kJ/mol. Natural charges were computed using NBO 3.0, as implemented in the Gaussian03 package.

Supporting Information (see also the footnote on the first page of this article): The DFT total energies, geometrical parameters, NBO atomic charges, and calculated geometries of BAEs **1**, **2**, **6**–**8**, **17**–**22**.

[1] a) G. Shoham, S. Cohen, R. M. Suissa, I. Agranat, in *Molecular Structure: Chemical Reactivity and Biological Activity* (Eds.: J. J. Stezowski, J.-L. Huang, M.-C. Shao), IUCr Crystallographic Symposia 2, Oxford University Press, Oxford, **1988**, pp. 290–312; b) P. U. Biedermann, J. J. Stezowski, I. Agranat, in *Advances in Theoretically Interesting Molecules* (Ed.: R. P. Thummel), vol. 4, JAI Press: Stanford, CN, **1988**, pp. 245–322; c) P. U. Biedermann, J. J. Stezowski, I. Agranat, *Eur. J. Org. Chem.* **2001**, 15–34.

[2] C. de la Harpe, W. A. Van Dorp, *Ber. Dtsch. Chem. Ges.* **1875**, *8*, 1048–1050.

[3] a) J. H. Day, *Chem. Rev.* **1963**, *63*, 65–80; b) E. D. Bergmann, *Prog. Org. Chem.* **1955**, *3*, 81–171; c) G. Kortüm, *Ber. Bunsen-Ges. Phys. Chem.* **1974**, *78*, 391–403; d) H. Bouas-Laurent, H. Dürr, *Pure Appl. Chem.* **2001**, *73*, 639–665.

[4] A. Samat, V. Lokshin, in *Organic Photochromic and Thermochromic Compounds* (Eds.: J. C. Crano, R. J. Guglielmetti), vol. 2, Plenum Press, New York, **1999**, p. 415.

[5] P. U. Biedermann, J. J. Stezowski, I. Agranat, *Chem. Eur. J.* **2006**, *12*, 3345–3354.

[6] a) H. Meyer, *Ber. Dtsch. Chem. Ges.* **1909**, *42*, 143–145; b) H. Meyer, *Monatsh. Chem.* **1909**, *30*, 165–177.

[7] D. L. Fanselow, H. G. Drickamer, *J. Chem. Phys.* **1974**, *61*, 4567–4574.

[8] a) Y. Hirshberg, *Compt. Rend.* **1950**, *231*, 903–904; b) G. Kortüm, W. Theilacker, V. Braun, *Z. Physik. Chem.* **1954**, *NF 2*, 179–196; c) T. Bercovici, R. Korenstein, K. A. Muszkat, E. Fischer, *Pure Appl. Chem.* **1970**, *24*, 531–565; d) E. Fischer, *Chem. Unserer Zeit* **1975**, *9*, 85–95; e) E. Fischer, *Rev. Chem. Intermed.* **1984**, *5*, 393–422; f) K. A. Muszkat in *The Chemistry of Quinonoid Compounds* (Eds.: S. Patai, Z. Rappoport), vol. 2, Wiley, Chichester, **1988**, pp. 203–224; g) W. H. Laarhoven in *Photochromism, Molecules and Systems* (Eds.: H. Dürr, H. Bouas-Laurent), Elsevier, Amsterdam, **1990**, pp. 270–313; h) *Organic Photochromic and Thermochromic Compounds* (Eds.: J. C. Crano, R. J. Guglielmetti), *Topics in Applied Chemistry*, vol. 1, *Photochromic Families*, vol. 2, *Physicochemical Studies, Biological Applications, and Thermochromism*, Plenum Press, New York, **1999**.

[9] B. L. Feringa, *Acc. Chem. Res.* **2001**, *34*, 504–513.

[10] a) K. Linde, G. Ramirez, C. D. Mulrow, A. Pauls, W. Weidenhammer, D. Melchart, *Brit. Med. J.* **1996**, *313*, 253–258; b) M. Philipp, R. Kohnen, K.-O. Hiller, K. Linde, M. Berner, *Brit. Med. J.* **1999**, *319*, 1534–1539.

[11] R. Herges, *Chem. Rev.* **2006**, *106*, 4820–4842.

[12] a) W. T. Grubb, G. B. Kistiakowsky, *J. Am. Chem. Soc.* **1950**, *72*, 419–424; b) W. Theilacker, G. Kortüm, G. Friedheim, *Ber. Dtsch. Chem. Ges.* **1950**, *83*, 508–519; c) Y. Hirschberg, E. Fischer, *J. Chem. Soc.* **1953**, 629–636; d) G. Kortüm, *Angew. Chem.* **1958**, *70*, 14–20; e) Z. R. Grabowski, M. S. Balasiewicz, *Trans. Faraday Soc.* **1968**, *64*, 3346–3353; f) Y. Tapuhi, O. Kalisky, I. Agranat, *J. Org. Chem.* **1979**, *44*, 1949–1952; g) T. Natsue, D. H. Evans, *J. Electroanal. Chem.* **1984**, *168*, 287–298.

[13] a) E. Harnik, *J. Chem. Phys.* **1956**, *24*, 297–299; b) E. Wasserman, R. E. Davis, *J. Chem. Phys.* **1959**, *30*, 1367; c) G. Kortüm, G. Bayer, *Ber. Bunsen-Ges. Phys. Chem.* **1963**, *67*, 24–28; d) R. Korenstein, K. A. Muszkat, E. Fischer, *Helv. Chim. Acta* **1970**, *53*, 2102–2109.

[14] P. U. Biedermann, J. J. Stezowski, I. Agranat, *Chem. Commun.* **2001**, 954–955.

[15] A. Levy, P. U. Biedermann, I. Agranat, *Org. Lett.* **2000**, *2*, 1811–1814.

[16] Yu. V. Zefirov, *Crystallogr. Rep. (Kristallografiya)* **1997**, *42*, 111–116.

[17] A. Levy, S. Cohen, I. Agranat, *Org. Biomol. Chem.* **2003**, *1*, 2755–2763.

[18] R. M. Suissa, Ph. D. Thesis, The Hebrew University of Jerusalem, Jerusalem, **1988** (in Hebrew).

[19] E. D. Bergmann, Y. Hirschberg, D. Lavie, *Bull. Soc. Chim. Fr.* **1952**, *19*, 268–270.

[20] A. F. A. Ismail, Z. M. El-Shafei, *J. Chem. Soc.* **1957**, 3393–3396.

[21] a) D. H. R. Barton, B. J. Wills, *J. Chem. Soc. Perkin Trans. 1* **1972**, 305–310; b) D. H. R. Barton, F. S. Guziec, I. Shahak, *J. Chem. Soc. Perkin Trans. 1* **1974**, 1794–1799.

[22] A. Schönberg, W. I. Awad, N. Latif, *J. Chem. Soc.* **1951**, 1368–1369.

[23] M. S. Raasch, *J. Org. Chem.* **1979**, *44*, 632–633.

[24] S. Scheibye, R. Shabana, S.-O. Lawesson, C. Roemming, *Tetrahedron* **1982**, *38*, 993–1001.

[25] M. Regitz, *Chem. Ber.* **1964**, *97*, 2742–2754.

[26] A. Levy, P. U. Biedermann, S. Cohen, I. Agranat, *J. Chem. Soc. Perkin Trans. 2* **2001**, 2329–2341.

[27] A. Schönberg, K. Junghans, *Chem. Ber.* **1962**, *95*, 2137–2143.

[28] CCDC-645716 to -645718 contain the supplementary crystallographic data for this paper. These data can be obtained free of charge from The Cambridge Crystallographic Data Centre via www.ccdc.cam.ac.uk/data_request/cif.

[29] P. A. Apgar, E. Wasserman, unpublished results (Allied Chemical), **1978**, quoted in ref. 1a.

[30] I. Agranat, Y. Tapuhi, *J. Org. Chem.* **1979**, *44*, 1941–1948.

[31] a) F. De Proft, P. Geerling, *Chem. Rev.* **2001**, *101*, 1451–1464; b) W. Koch, M. C. Holthausen, *A Chemist Guide to Density Functional Theory*, Wiley-VCH, Weinheim, **2000**.

[32] S. Pogodin, I. D. Rae, I. Agranat, *Eur. J. Org. Chem.* **2006**, 5059–5068.

[33] P. George, M. Trachtman, C. W. Bock, A. M. Brett, *Theor. Chim. Acta* **1975**, *38*, 121–129.

[34] E. D. Bergmann, *Isomerism and Isomerization of Organic Compounds*, Interscience Publishers, New York, **1948**, p. 48.

[35] A. Ault, R. Kopet, A. Serianz, *J. Chem. Educ.* **1971**, *48*, 410–411.

[36] *Gaussian 03*, Revision C.02, M. J. Frisch, G. W. Trucks, H. B. Schlegel, G. E. Scuseria, M. A. Robb, J. R. Cheeseman, J. A. Montgomery Jr, T. Vreven, K. N. Kudin, J. C. Burant, J. M. Millam, S. S. Iyengar, J. Tomasi, V. Barone, B. Mennucci, M. Cossi, G. Scalmani, N. Rega, G. A. Petersson, H. Nakatsuji, M. Hada, M. Ehara, K. Toyota, R. Fukuda, J. Hasegawa, M. Ishida, T. Nakajima, Y. Honda, O. Kitao, H. Nakai, M. Klene, X. Li, J. E. Knox, H. P. Hratchian, J. B. Cross, C. Adamo, J. Jaramillo, R. Gomperts, R. E. Stratmann, O. Yazyev, A. J. Austin, R. Cammi, C. Pomelli, J. W. Ochterski, P. Y. Ayala, K. Mo-

rokuma, G. A. Voth, P. Salvador, J. J. Dannenberg, V. G. Zakrzewski, S. Dapprich, A. D. Daniels, M. C. Strain, O. Farkas, D. K. Malick, A. D. Rabuck, K. Raghavachari, J. B. Foresman, J. V. Ortiz, Q. Cui, A. G. Baboul, S. Clifford, J. Cioslowski, B. B. Stefanov, G. Liu, A. Liashenko, P. Piskorz, I. Komaromi, R. L. Martin, D. J. Fox, T. Keith, M. A. Al-Laham, C. Y. Peng, A. Nanayakkara, M. Challacombe, P. M. W. Gill, B. Johnson, W. Chen, M. W. Wong, C. Gonzalez, J. A. Pople, Gaussian, Inc., Wallingford CT, **2004**.
[37] A. D. Becke, *J. Chem. Phys.* **1993**, *98*, 5648–5652.
[38] C. Lee, W. Yang, R. G. Parr, *Phys. Rev. B* **1988**, *37*, 785–789.
Received: May 8, 2007
Published Online: August 30, 2007

